Open Archive TOULOUSE Archive Ouverte (OATAO)

OATAO is an open access repository that collects the work of Toulouse researchers and makes it freely available over the web where possible.

Any correspondance concerning this service should be sent to the repository administrator: staff-oatao@inp-toulouse.fr.

Uptake and Release of Double-Walled Carbon Nanotubes by Mammalian Cells

By *Vera Neves, Elena Heister, Sara Costa, Carmen Tîlmaciu, Ewa Borowiak-Palen, Cristina E. Giusca, Emmanuel Flahaut, Brigitte Soula, Helen M. Coley, Johnjoe McFadden,* and *S. Ravi P. Silva**

Efforts to develop carbon nanotubes (CNTs) as nano-vehicles for precise and controlled drug and gene delivery, as well as markers for in vivo biomedical imaging, are currently hampered by uncertainties with regard to their cellular uptake, their fate in the body, and their safety. All of these processes are likely to be affected by the purity of CNT preparation, as well as the size and concentration of CNTs used, parameters that are often poorly controlled in biological experiments. It is demonstrated herein that under the experimental conditions of standard transfection methods, DWNTs are taken up by cultured cells but are then released after 24 h with no discernable stress response. The results support the potential therapeutic use of CNTs in many biomedical settings, such as cancer therapy.

1. Introduction

An important characteristic of functionalized carbon nanotubes (CNTs) is their ability to cross cell membranes.[1,2] The uptake of CNTs has been previously described to occur via two major pathways. One method describes nanotubes as "nanoneedles" that have the capability to penetrate cell membranes,[3] whereas the second method refers to an active uptake via clathrin mediated endocytosis.[1]

As controversy regarding the mechanism of uptake of CNTs persists, the final fate of nanotubes has been largely open to speculation. The previously described "nanoneedle" carbon nanotubes internalization has been proposed to lead to perinuclear accumulation with no effect on cell viability.[4] Conversely, CNTs bio-functionalized with biomolecules, such as DNA, have been shown to be subjected to exocytosis by NIH-3T3 fibroblast cells in a study carried out by Jin et al.[5]

Previously, the most commonly used technique to visualize the uptake of CNTs focused on visualizing internalization facilitated via the covalent linking of a visible-wavelength fluorophore.[1–4,6–7] However, when considering this approach, it is important to consider that: chemical linkages must resist enzymatic cleavage (due to activity in cytosolic compartments); the emission from the visible-wavelength fluorophore must be detected above background endogenous fluorescence; and chemical processing of nanoparticles may dramatically change their ultimate biological fate. As an alternative to the linking of fluorophores, it is possible to use the unique NIR intrinsic fluorescence associated with CNTs. The latter property is considered as being advantageous for use in biological systems, since there are minimal background signals associated with autofluorescence from cells, tissues, and other biological molecules in this spectral range, as this property has largely been shown to be confined to the visible spectral range.[8] Raman spectroscopy is a multi-purpose, rapid (~1 min per spectrum) non-destructive technique that operates at normal ambient (room temperature) (~300 K) and pressure conditions, and uses readily available Raman characterization instrumentation.[9] Due to the electronic structure and diameter of CNTs, strong resonance-enhanced Raman bands are produced at 150–300, 1590–1600, and approximately 2600 cm^{-1} away from the excitation wavelength.[10] The first of these, referred to as the radial breathing mode (RBM), is caused by uniaxial vibrations and depends linearly on the nanotube diameter. The RBM is then followed by the disorder-induced D-band, the tangential mode (or G-band), which is caused by stretching along the C–C bonds of graphene[10–12] and, finally, the G′-band, a two-phonon mode.[10]

Besides the fate of CNTs, the major challenge of using them in biological systems is assessing whether CNTs are inherently cytotoxic.[13–22] At present, there are roughly as many publications reporting no apparent cytotoxicity,[3,6,8,20,23–36] as there are reporting varying degrees of significant loss of cellular viability associated with CNTs.[37–50] Two major considerations in this area are how the CNTs are presented and another their purity and concentration of the carbon nanotubes. For example,

[*] V. Neves, E. Heister, C. E. Giusca, Prof. S. R. P. Silva
     Nanoelectronics Centre
     Advanced Technology Institute
     University of Surrey
     Guildford, GU2 7XH (UK)
     E-mail: S.Silva@surrey.ac.uk
     V. Neves, E. Heister, Dr. H. M. Coley, Prof. J. McFadden
     Faculty of Health and Medical Sciences
     University of Surrey
     Guildford, GU2 7XH (UK)
     Dr. S. Costa, Dr. E. Borowiak-Palen
     West Pomeranian University of Technology in Szczecin
     Institute of Chemical and Environment Engineering
     Piastów 17, 70–310 Szczecin (Poland)
     C. Tîlmaciu, Dr. E. Flahaut, Dr. B. Soula
     Université de Toulouse, UPS/INP/CNRS
     Institut Carnot CIRIMAT
     118 route de Narbonne, 31062 Toulouse, Cedex 9 (France)

pulmonary toxicity of SWNT has been established when large doses of dry, unpurified SWNT have been blown into lungs of rats.[42,48–49] This method of presentation is not relevant to the small measured doses of CNTs that would be used as chemotherapy and drug delivery systems. In fact, the biodistribution of chemically modified SWNT injected into mice or rabbits was studied recently, and the CNTs were reported to be rapidly excreted with no evidence of toxicity.[24,51–52] The purity of CNT preparation is a crucial consideration in their use as bio-nano agents. Many methods of CNT synthesis use metal catalysts that are known to be toxic. Such impurities, and other carbonaceous impurities, must be removed from the samples in order to reach correct and safe conclusions regarding the inherent toxicity of CNTs. At present the data is unclear as to what contribution these factors may have made to the various reported toxicological profiles of CNTs.

Here, we study the cellular uptake and release of DWNTs by Raman spectroscopy using single-cell mapping and spectroscopy analysis of whole cell lysates incubated with oxidized double-walled carbon nanotubes (ox DWNTs) wrapped with RNA, and evaluate their safety by examine cells for any sign of cellular stress response to CNT uptake.

2. Results and Discussion

Our group has previously demonstrated the use of RNA-wrapping for purification and functionalization of CNTs.[53,54] This study is designed to investigate the uptake and release of double-walled carbon nanotubes (DWNTs) by cultured human cancer cells. However, detection of DWNTs intracellularly is non-trivial as (in their pure form) they consist of only carbon atoms linked by covalent C = C double bonds, and thus are not easily discernable from biological complexes present in the cellular milieu using standard spectroscopic methods. The small size and low contrast of CNTs also makes them difficult to distinguish from cellular structures by microscopy techniques. Direct and label-free mapping of CNTs inside living cells has recently been demonstrated using their characteristic intrinsic near-infrared fluorescence[8,55–56] and Raman scattering.[56] However, a marked decrease in the intrinsic fluorescence intensity of CNTs has been observed[56] following protracted periods (8 d) in culture, whereas the Raman signal is stable over the same time period. The aim of this study was to further investigate cellular uptake and fate of DWNTs. **Figure 1c** and 1d present the Raman spectra of pristine and RNA-wrapped oxidized double-walled carbon nanotubes (DWNT and oxDWNT-RNA, respectively) with two different laser wavelengths (473 and 785 nm, respectively), which generate spectra with the typical peaks expected for DWNTs. The spectra were very similar for the oxDWNT-RNA and the pristine sample, indicating that their spectral properties have not changed as a consequence of functionalization. Transmission electron microscopy (TEM) and atomic force microscopy (AFM) demonstrated that oxidized samples wrapped with RNA (Figure 1a and 1b) were more de-bundled and individualised, with length distributions ranging from 200 nm to 2 μm. The size distribution and RNA wrapping of DWNT is not the primary study of this report and hence is described elsewhere.[54]
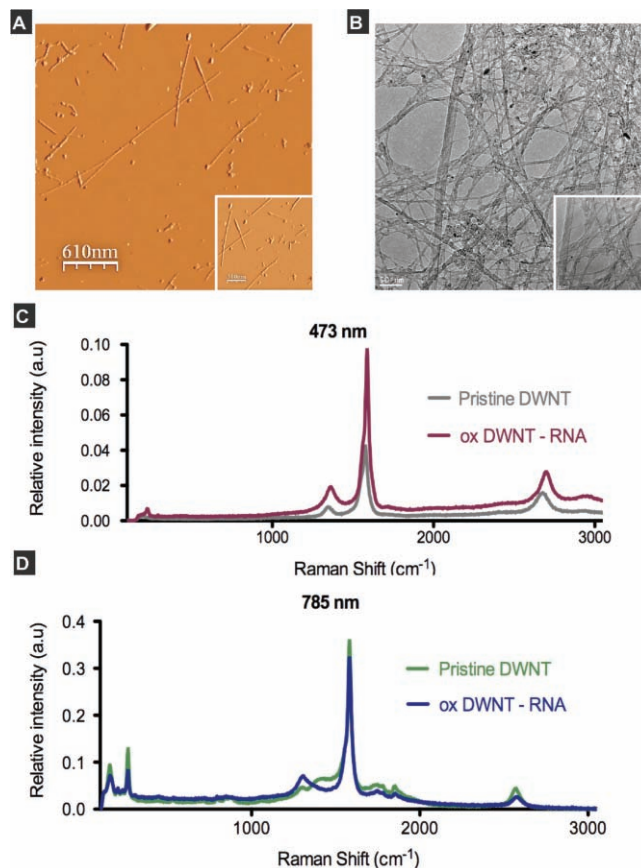

Figure 1. Structural characterization of double-walled carbon nanotubes (DWNT) by AFM, TEM and Raman spectroscopy. A) and B) Surface analysis of RNA-wrapped oxidized DWNTs (oxDWNT-RNA) by AFM and TEM, respectively. oxDWNTs-RNA were found to range between 200 nm and 2 μm in length (data not shown). C) and D) Raman spectrum of pristine and oxDWNT-RNA at different laser energies: 473 and 785 nm. Intense bands can be seen at 120–350 cm^{-1} for the radial breathing modes (RBM); at ~1590 cm^{-1} for the tangential G-band; at ~1350 cm^{-1} for the disorder-induced D band, and at ~2900 cm^{-1} for its second-order harmonic, the G' band.[10]

2.1. Cellular Uptake and Release of DWNT by Raman Spectroscopy

2.1.1. RBM Mapping of Single Cells

The radial breathing mode (RBM) is a unique phonon mode that depends on the nanotube diameter and thereby allows tubes of different diameters to be monitored as they accumulate inside cells. Human cells were incubated with DWNTs to allow uptake. The same distribution of RBMs with peaks at 156, 205, 230 and 266 cm^{-1} were detected in pristine DWNTs, DWNTs inside PC3 cells (human prostate adenocarcinoma) and extracellular DWNTs, indicating that there was no selectivity of DWNTs according to the cellular system (**Figure 2a**). Figure 2b illustrates the distribution of nanotubes inside PC3 cells using the RBM peak at approximately 260 cm^{-1} (corresponding to a tube diameter of 0.9 nm, the strongest peak in the sample) for a single cell. Figure 2c illustrates the distribution of nanotubes
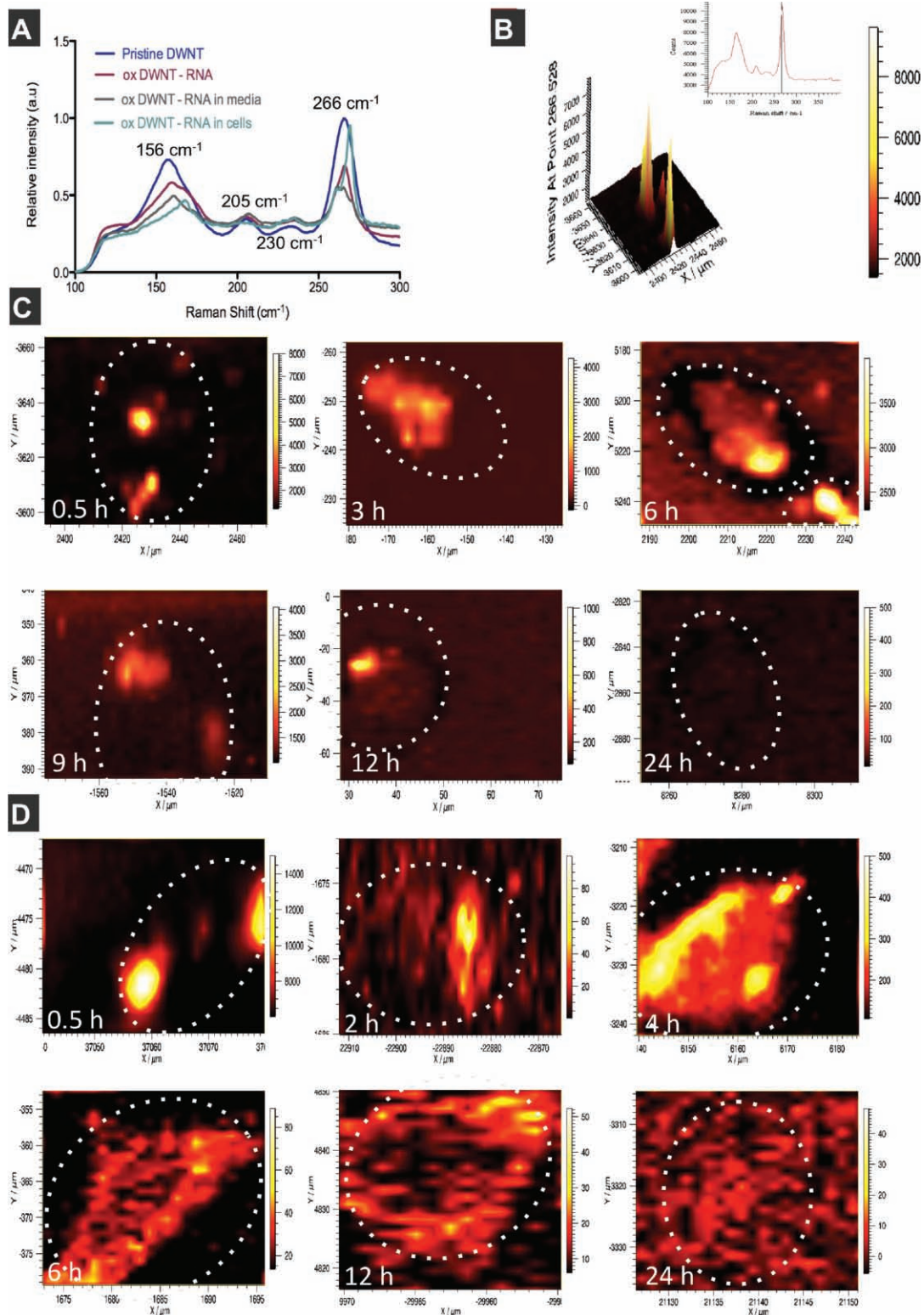
Figure 2. Single cell mapping of PC3 and HeLa cells exposed to DWNTs. RBMs were used to track DWNTs in cells. As displayed, a uniform distribution of diameters is obtained in all different conditions: pristine nanotubes, oxidized DWNT wrapped with RNA, and the same oxDWNT-RNA in cell medium and inside cells (A). A grid was defined on a single cell, and a map obtained by collecting spectra with 1 min exposure time and moving the sample with increments of 1 μm (spectral resolution of 4 cm⁻¹). Data analysis was performed at ~260 cm⁻¹ as illustrated by RBM spectra and the 3D map (B). (C and D) 2D mapping at various time points from 0.5 h to 24 h in PC3 (C) and HeLa (D). The broken line in the different figures from 0.5 to 24 h crudely represents the boundaries of the cell and demonstrates that a high intensity is confined to the cell, an effect not observed for media alone.

inside PC3 single cells over a 24 h time course using the same RBM peak. Figure 2d displays Raman analysis of HeLa cells (human cervical carcinoma), demonstrating similar dynamics for both cell lines. In both model systems, the highest intensity was obtained after 0.5 h, possibly corresponding to localization of DWNTs inside endosomes. This was followed by a reduced intensity at 3 and 9 h, which was more diffused throughout the cell, indicating that DWNTs had been released from their initial site of sequestration. After 12 h the intensity dropped in magnitude 4-fold, until finally at 24 h no distinct RBM at 260 cm^{-1} could be detected. The percentage of cells containing DWNTs was estimated on the basis of whether CNT Raman peaks could be detected (see the Supporting Information, Table S1). The highest percentage of cells with nanotubes, was 50%, at 3 h. This proportion decreased by approximately 3-fold at 12 h and 5-fold by 24 h. Parallel experiments (see the Supporting Information, Figure S1) examining the uptake of fluorescently labeled DWNTs by confocal microscopy were used to examine the Z-plane localization of DWNTs and clearly demonstrated that the majority of nanotubes were located intracellularly, rather than being on the surface, of the cells. Finally, viable cells were counted and no significant cell death was detected during the incubation period.

Figure 3. Temporal evaluation of DWNT uptake by PC3 and HeLa whole cell lysates. A) Raman spectrum at different time points obtained for PC3 after exposure to RNA-wrapped oxidized DWNT (oxDWNT-RNA). CNT features are visualised at 1350, 1590 and 2700 cm^{-1} with D, G and G' bands and cellular constituents at 1090, 1450, 1660 and 2900 cm^{-1}. Spectra were normalized such that in each data set 100% represents the sum of all values in the data set. B) Area under the curve (AUC) of G band intensity at the various time points for PC3 and HeLa cells. (∗∗∗ indicates p < 0.0001 and ∗ p < 0.05, one-way anova test)

2.1.2. G-Band Intensity on Whole Cell Lysates

The observed reduction in Raman signal over the 24 h time-course in individual cells could be due to diffusion of discrete concentrations of DWNTs (for instance, in endosomes) throughout the entire volume of the cell, or by the loss of DWNTs from the cell. To distinguish between these two possibilities, we lysed the cells and performed Raman spectroscopy on small samples of cell lysate. **Figure 3a** shows the Raman spectra in PC3 cells at various time points. The CNT-characteristic D-, G- and G'-Raman bands were detected; however, in addition four other peaks were observed at approximately 1090, 1450, 1660 and 2900 cm^{-1}, which previous studies[57–59] have associated with cellular constituents. The CNT-specific G-band at 1590 cm^{-1} corresponds to the LO phonon breathing mode of CNTs that is characteristic of all sp^2 carbon materials[60] and is therefore a useful tool to quantify DWNTs. Examination of Figure 3b, in both PC3 and HeLa cell lines, demonstrates a maximal intensity at 3 h (statistically significant $P < 0.0001$) and minimum at 24 h ($P > 0.05$), corresponding to the times for maximum uptake and release, respectively, measured in individual cells (Figure 2 and Table S1 in the Supporting Information). The observed reduction of the Raman signal in cell lysates indicates that the DWNTs are being lost from the cell, rather than merely diffusing through the cell. (We also investigated whether addition of cell lysate changed the G-band intensity of isolated DWNTs, however no change was observed, see
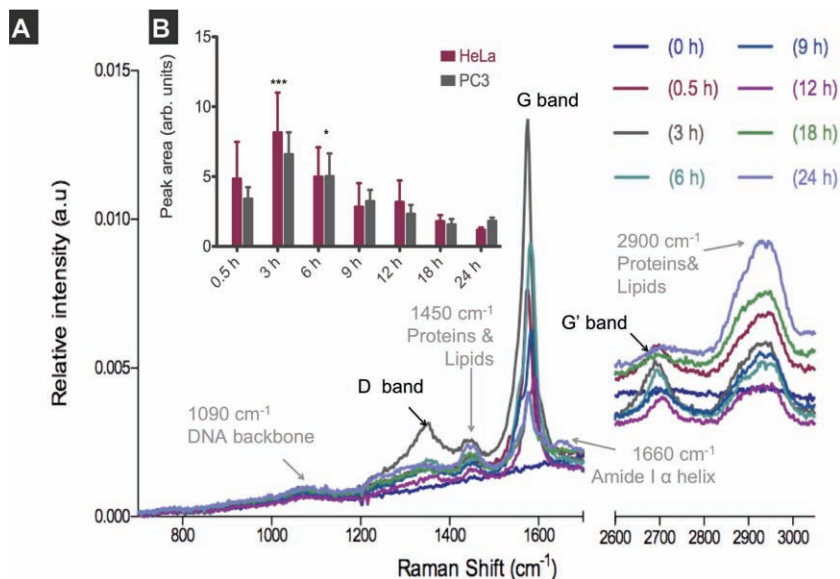
the Supporting Information, Figure S5). The G-band intensity was calibrated by reference to quantified samples of pure DWNTs and used to provide an estimate of CNT concentration within the PC3 cell lysate. Using an approximate cell volume of 5.75×10^{-9} µL, the concentration of DWNTs inside cells was estimated to be 33.63×10^{-6} pg per cell (at peak concentration after 3 h incubation, see the Supporting Information, Table S2). The concentration of DWNTs in cell lysates (5.85 µg mL^{-1}) was approximately 20% of the initial concentration in the tissue culture medium (see the Supporting Information, Table S2), indicating that uptake may be limited during the 3 h of the incubation with DWNTs. AFM analysis of PC3 cell lysate at 3 h revealed that the DWNT internalized size ranged between 100 nm and 1.2 µm, indicating negligible size selectivity during uptake.

The D-band in the Raman spectra corresponds to defects in the CNT wall and so the ratio of this to the G-band (I_D/I_G ratio) was used to monitor the integrity of the DWNTs.[61] This ratio is plotted in **Figure 4a**, where it is apparent that it increases, roughly linearly, during the course of the experiment (note that the first data point in Figure 4a corresponds to 6 h incubation with the DWNTs, as this was the first data-point after which the cells were washed to remove extracellular DWNTs). These results suggest that the nanotubes are being modified or degraded during their incubation inside cells. However, the D-peak is relatively weak and therefore difficult to quantify. So, to investigate this phenomenon further, the RBM obtained from single cell mapping was also analyzed. Only frequencies corresponding to wall diameters of 0.9 and 1.58 nm were considered, as these were noted to be the dominant resonances under the wavelength
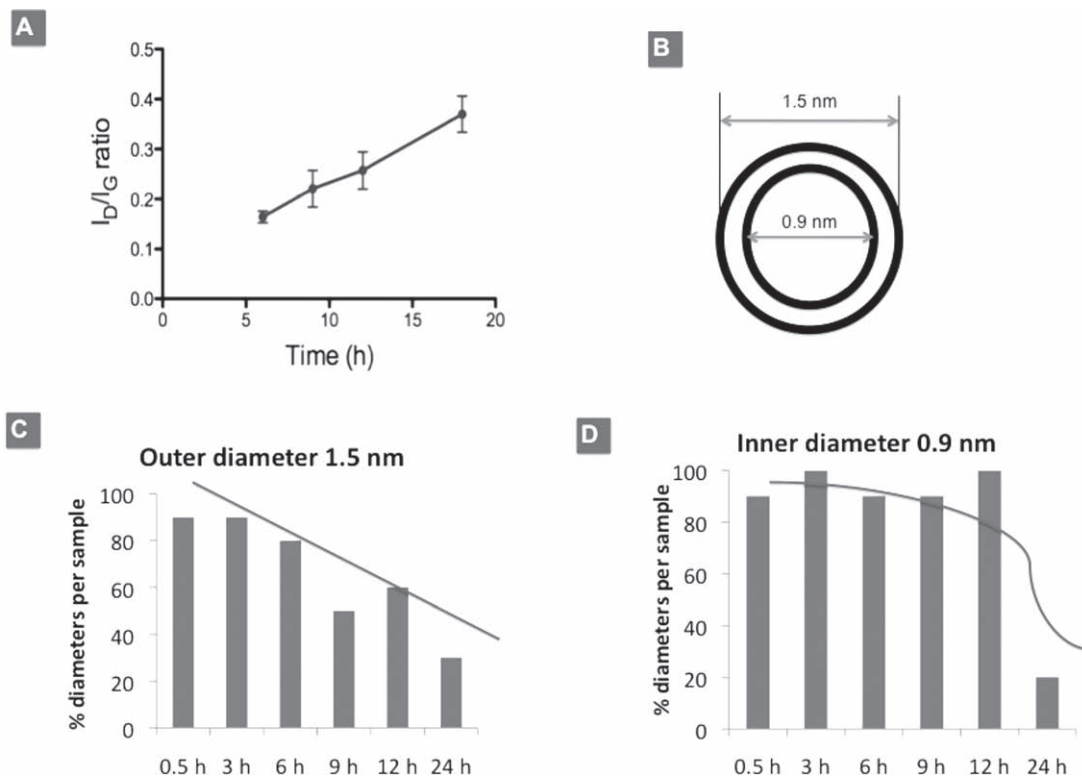
Figure 4. Increase in defects on DWNT walls. A) Raman D/G intensity ratio for carbon nanotubes in PC3 cells at different time points from 6 to 18 hours (3 h was the point where exposure to nanotubes ended and cellular release of DWNTs started to take place. Due to the decrease in the signal-to-noise ratio at 24 hours, this time point was excluded from the data set). Error bars were calculated using the standard mean error (n = 6). B) Conformation of a DWNT (matching interlayer spacing of CNTs of 0.344 nm). C) 1.58 nm diameter distribution over time inside cells. D) 0.9 nm diameter distribution over time inside cells.

of Raman excitation. We propose that the 1.58 nm diameter walls detected by Raman RBM corresponds to the outer walls and the 0.9 nm walls to the inner walls of the DWNTs in our samples (Figure 4b). This implies an interlayer spacing of 0.344 nm, which corresponds to the observed wall spacing reported in other studies.[62] A sample collection of 10 spectra were obtained and analysed. The percentage of distribution of the signals over time is displayed in Figure 4c and d. For the signal corresponding to a diameter of 1.58 nm there is a linear decrease over the 24 h period, suggesting that the CNTs are either being lost or defects are accumulating to the outer wall over time. However, the peak corresponding to the 0.9 diameter wall distribution remains constant until 12 h, suggesting that, up to this time-point, the tubes are not extruded from cells in significant quantities. The subsequent sharp decrease in the inner wall signal at 24 h could be due to loss of CNTs from the cell or defects accumulating in the inner CNT. However, even at this time-point the peak corresponding to the outer wall is still apparent in 30% of samples, so we consider it is more likely that the CNTs are being lost from the cell at this time-point. Additionally, in vitro studies by Allen et al.[63] found significant degradation of SWNTs, but only after 12 weeks of incubation at 4 °C with low concentrations of H_2O_2 and peroxidase. Also, Liu et al.[64] incubated SWNTs with a chemical mixture simulating the phagolysosomal compartment and found that only oxidized SWNTs were significantly degraded after 90 d. Together, these results suggest that the DWNTs are probably being lost from cells during the 24 h incubation in our experiments, rather than being entirely degraded.

2.1.3. Cell Biochemistry Analysis by Raman Over a 24 h Timeframe on Cells Exposed to DWNTs and Controls

To monitor the response of the cell to DWNTs, Raman bands corresponding to cell constituents such as DNA/RNA, proteins and lipids were monitored at approximately 1090, 1450, 1660, and 2900 cm^{-1} (Figure 3a).[57–59] No change was observed in the band at 1090 cm^{-1} corresponding to the DNA O–P–O backbone stretching, which is associated with cell death and is associated with breaking of the phosphodiester bonds in DNA.[65] Similarly, no changes in Raman peaks at around 1 660 cm^{-1} (corresponding to amide I vibrations in proteins and C=C in lipids[66]); at 2800–3100 cm^{-1} (corresponding to C–H stretching vibration in protein and lipids); 2930 to 2950 (corresponding to symmetric and anti-symmetric CH$_3$ stretch vibrations in proteins and lipids); and near 1440 cm^{-1} (corresponding to C–H deformation bands in lipids and proteins),[59] were detected (see the Supporting Information, Figure S4). Additionally, overall protein levels were monitored by gel electrophoresis, which confirmed that no significant change to protein levels occurred during the incubation (see the Supporting Information, Figure S5).
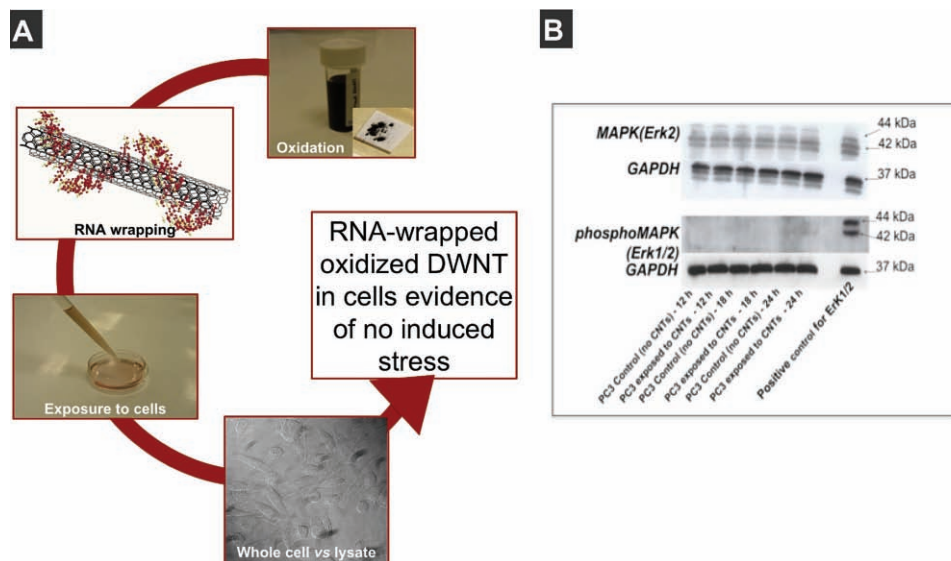
Figure 5. Cellular interactions to DWNTs. A) Overview diagram of experimental set up. B) expression of non-phosphorylated MAPK (Erk 2) and control of loading sample with GAPDH (top); phosphorylated MAPK (Erk 1/2) and control of loading sample with GAPDH (bottom), on PC3 cells exposed to carbon nanotubes and controls.

Together, these results indicate that the uptake of DWNTs did not induce any detectable biochemical changes in the cell.

2.1.4. Evaluation of Stress Response Over a 24 h Timeframe on Cells Exposed to DWNT and Controls

As previously stated, cell viability was unchanged during the course of the experiment, indicating no direct effect of DWNTs on cell mortality. However, we also examined cells for any sign of cellular stress response as a consequence of CNT uptake. The mitogen-activated protein kinase (MAPK) pathways are activated by diverse extracellular and intracellular stimuli, including peptide growth factors, cytokines, hormones, and various cellular stressors, such as oxidative stress and endoplasmic reticulum stress. The extracellular signal-related kinase 1 (Erk 1, 44 kDa protein – p44) and 2 (Erk 2, 42 kDa protein – p42) are components of the MAPK family. Their activation requires phosphorylation by upstream kinases. We therefore measured the phosphorylation state of these factors by immunoblotting. In **Figure 5b**, the non-phosphorylated form of Erk p44/p42 is expressed constitutively and is hence detected in all samples at similar levels. However, the phosphorylated activated form of Erk p44/p42 was detected only in the positive control sample, indicating no detectable activation of the MAPK pathway during the experiment.

3. Conclusions

Herein, we show evidence, for the first time, that DWNTs functionalized by oxidation and RNA-wrapping can be taken up in vitro and then subsequently released by cells over a 24 h time period. The cellular handling of CNTs as visualized in our studies is certainly dependent on the functionalization method,

RNA-wrapping and incubation conditions, as seen following 3 h of exposure to oxDWNT-RNA and consequent release over a 24 h time course. Jin et al.[5] reported the first evidence for exocytosis of DNA-wrapped CNTs by using single particle tracking (SPT). However, in their study they followed the cells for only 2 h after washing, whereas we monitored cells for 24 h, thereby observing a peak of uptake at 3 h followed by an almost complete loss of CNTs from the cells. Jin et al.[5] demonstrated that the rate of exocytosis closely matches the rate of endocytosis;[5] however, in our study we demonstrate that nearly all of the CNTs are eventually released from the cells. This was shown with both studies of individual cells, but also with lysates derived from cell populations. Furthermore, we were also able to examine cell toxicity and activation of stress responses and could find no evidence of either effect following DWNT uptake and release. However, a novel feature of these studies was that changes in I_D/I_G ratios and RBM modes were observed during the course of incubation of cells with DWNTs. The source of these changes is currently uncertain, but suggests that the outer walls of DWNTs are being modified during their passage through the cells.

In conclusion, our results demonstrate that DWNTs prepared appropriately and supplied in reasonable quantities are non-toxic for human cells and potentially suitable for medical applications.

4. Experimental Section

Preparation of Biofunctional Carbon Nanotubes: Double-walled carbon nanotubes (DWNTs) synthesised by the CCVD technique[67] were purified in concentrated nitric acid and oxidized in a mixture of nitric and sulfuric acid.[68] After oxidation, nanotubes were sterilized by autoclaving at 121 °C for 1 h and were maintained under sterile conditions for the duration of the experiment. In a second step, the DWNTs were biofunctionalised

by wrapping with RNA in a proportion of 1:1 (w/w).[53] Complexes were formed by sonication in a water bath for 60 min. To remove excess of RNA, the suspension of oxidized DWNTs wrapped with RNA (oxDWNT-RNA) was filtered using a 100 kDa filter devices (Amicon Ultra-4 centrifugal filter devices Millipore, supplied by fisher UK Ltd) and then resuspended in deionised water. The concentration of the complexes was determined by total weight after oxidation, not accurate concentration of DWNTs but useful estimation of the material exposed to cells. The final supernatant was analysed by atomic force microscopy (AFM) topography measurements and transmission electron microscopy (TEM).

Raman Mapping of Single Cells: PC-3 (human prostate adenocarcinoma cells) and HeLa (human cervical carcinoma cells) in culture were used as model cellular systems for the present study. PC-3 cells (obtained from Promochem, Teddington, UK) were cultured in RPMI-1640 medium supplemented with 10% fetal bovine serum (FBS), 2×10^{-3} M Glutamax and 1% penicillin-streptomycin (all obtained from Invitrogen, Paisley, UK). HeLa cells (obtained from Promochem, Teddington, UK) were cultured in MEM medium supplemented with 10% fetal bovine serum (FBS), 1% non-essential amino acids and 1% penicillin-streptomycin (all obtained from Invitrogen, Paisley, UK). Cells were cultured in 35 mm sterile petri dishes (Nunc) containing glass coverslips. When the cells reached 80% confluence, they were incubated for 0.5 to 24 h with oxidized DWNTs wrapped with RNA at a concentration of approximately 30 μg mL^{-1} diluted in Opti-MEM serum-free culture medium (Invitrogen). After 3 h incubation, the remaining samples were washed twice with cold, sterile PBS and fresh medium containing serum and antibiotics was added. The release of CNTs from the cells was monitored for another 21 h. At each time point, the medium was removed and the cells were washed several times with PBS, as before. Cells were subsequently fixed with 4% paraformaldehyde solution (Sigma Aldrich, UK) to prevent morphological and chemical changes during acquisition. Finally, the sample was again washed with PBS and slides mounted and hermetically sealed using nail lacquer. Raman mapping was performed using a Renishaw InVia Raman microscope, E_{laser} = 1.59 eV (785 nm wavelength). Radial breathing modes were used to map the intensity of DWNTS in cells, RBMs peaks were acquired at 156, 205, 230 and 266 cm^{-1}. Applying the equation $\omega_{RBM} = 248/d_t$, where ω_{RBM} is the RBM frequency in cm^{-1} and d_t the diameter in nm,[69] it was possible to extrapolate the diameters present in the mixture. The diameters in the sample ranged from: 0.9 to 1.1 and 1.2 to 1.58 nm, with 0.9 and 1.58 nm being the most abundant (data not shown). The diameter of 0.9 nm was used for all data analysis.

Raman Spectroscopy of Whole Cell Lysates: PC-3 and HeLa cells were grown in medium as described above and cultured in 25 cm^2 tissue culture flasks until they reached 80% confluence. At this point, they were incubated for various times ranging from 0.5 to 24 h with RNA-wrapped oxidized DWNT (around 30 μg mL^{-1}) diluted in serum-free Opti-MEM medium. After 3 h incubation, the remaining samples were washed twice with PBS and then with fresh medium containing serum and antibiotics. At each time point, the medium was removed from the cells, followed by several washes with PBS. The cells were subsequently trypsinized, washed with cold PBS and ruptured via hypotonic shock using a lysis buffer (Tris buffer containing 50×10^{-3} M Tris HCl and 150×10^{-3} M NaCl at pH 7.5 and additionally 1% NP-40, 0.2% SDS, 1×10^{-3} M phenylmethanesulfonyl fluoride (PMSF), 10 μg mL^{-1} aprotinin, 10 μg mL^{-1} leupeptin, 1×10^{-3} M sodium orthovanadate (Na$_3$VO$_4$) as cellular protease inhibitors. After lysing, suspensions were spun down (500g, 10 min at 4 °C) to remove nuclei and unbroken cells and supernatants were used to evaluate the DWNT content. For Raman measurements, a droplet of cell lysate (4 μL) was allowed to dry on a glass slide. Spectra of samples were recorded using the E_{laser} = 2.64 eV (473 nm wavelength) of an NT-MDT NTEGRA Spectra Probe NanoLaboratory inverted configuration microscope.

Protein Quantification and SDS Polyacrylamide Gel Electrophoresis: Protein quantification was performed according to instructions in the manual of the DC (detergent compatible) protein assay (Bio-Rad Laboratories, UK). A standard curve was prepared with BSA (0.2–1.5 mg mL^{-1}).

Protein/sample from cell lysates were electrophoresed on SDS-polyacrylamide gel electrophoresis gels (Novex, Invitrogen, UK) with subsequent coomassie staining for 2 h.

Concentration of DWNTs per Cell: G-band intensity was determined for different concentrations of DWNTs (93.50, 46.75, 23.37, 11.69, 5.84, and 2.92 μg mL^{-1}). Concentration was determined by total weight of functionalized DWNTs, oxDWNTs-RNA). A logarithmic fit was used to determine the equation that permits calculating the concentration in the whole cell lysates. Finally, an estimation of cell volume[70] was used to determine the concentration of DWNTs per cell.

Western Blotting: Whole-cell lysates were obtained by trypsinizing the monolayer of adherent cells and washing with PBS at 4 °C. Cell pellets were then subjected to osmotic rupture in hypotonic detergent-based buffer (1×10^{-3} M PMSF, 1×10^{-3} M NaVO$_4$, 2 μg mL^{-1} aprotinin, and 2 μg mL^{-1} leupeptin as protease inhibitors, 0.150 M NaCl in 0.050 M Tris buffer, 0.2% SDS, 1% Nonidet P-40, pH 7.5) and 50 μg of protein/sample were then electrophoresed on SDS-polyacrylamide gel electrophoresis gels (Novex, Invitrogen, UK) with subsequent transfer blotting. Membranes were incubated overnight at 4 °C with primary antibodies to MAPK, or phospho-MAPK (Cell signaling technology, UK). After washing, membranes were incubated with a secondary horseradish peroxidase-linked appropriate species antibody preparation at room temperature for 1 h with chemiluminescence used for visualization. After the probing of each membrane with the primary antibody of choice, the membrane was stripped and re-probed using a GAPDH antibody (Sigma Aldrich, UK) to act as a loading control.

Supporting Information

Supporting Information is available from the Wiley Online Library or from the author.

Acknowledgements

[1] N. W. S. Kam, T. C. Jessop, P. A. Wender, H. J. Dai, *J. Am. Chem. Soc.* **2004**, *126*, 6850.

[2] D. Pantarotto, J. P. Briand, M. Prato, A. Bianco, *Chem. Commun.* **2004**, 16.

[3] K. Kostarelos, L. Lacerda, G. Pastorin, W. Wu, S. Wieckowski, J. Luangsivilay, S. Godefroy, D. Pantarotto, J. P. Briand, S. Muller, M. Prato, A. Bianco, *Nat. Nanotechnol.* **2007**, *2*, 108.

[4] L. Lacerda, G. Pastorin, D. Gathercole, J. Buddle, M. Prato, A. Bianco, K. Kostarelos, *Adv. Mater.* **2007**, *19*, 1789.

[5] H. Jin, D. A. Heller, M. S. Strano, *Nano Lett.* **2008**, *8*, 1577.

[6] N. W. S. Kam, H. J. Dai, *J. Am. Chem. Soc.* **2005**, *127*, 6021.

[7] V. Raffa, G. Ciofani, S. Nitodas, T. Karachalios, D. D'Alessandro, M. Masini, A. Cuschieri, *Carbon* **2008**, *46*, 1600.

[8] P. Cherukuri, S. M. Bachilo, S. H. Litovsky, R. B. Weisman, *J. Am. Chem. Soc.* **2004**, *126*, 15638.

[9] A. Jorio, R. Saito, J. H. Hafner, C. M. Lieber, M. Hunter, T. McClure, G. Dresselhaus, M. S. Dresselhaus, *Phys. Rev. Lett.* **2001**, *86*, 1118.

[10] R. D. Saito, G. Dresselhaus, *Physical Properties of Carbon Nanotubes*, Imperial College Press, London **1998**.

[11] M. S. Strano, S. K. Doorn, E. H. Haroz, C. Kittrell, R. H. Hauge, R. E. Smalley, *Nano Lett.* **2003**, *3*, 1091.

[12] S. K. Doorn, D. A. Heller, P. W. Barone, M. L. Usrey, M. S. Strano, *Appl. Phys. A: Mater. Sci. Proc.* **2004**, *78*, 1147.

[13] G. Oberdorster, A. Maynard, K. Donaldson, V. Castranova, J. Fitzpatrick, K. Ausman, J. Carter, B. Karn, W. Kreyling, D. Lai, S. Olin, N. Monteiro-Riviere, D. Warheit, H. Yang, *Part Fibre Toxicol* **2005**, *2*, 8.

[14] A. Nel, T. Xia, L. Madler, N. Li, *Science* **2006**, *311*, 622.

[15] C.-w. Lam, J. James, R. McCluskey, S. Arepalli, R. Hunter, *Crit. Rev. Toxicol.* **2006**, *36*, 189.

[16] B. J. Panessa-Warren, J. B. Warren, S. S. Wong, J. A. Misewich, *J. Phys.: Condens. Matter* **2006**, *18*, 2185.

[17] N. A. Monteiro-Riviere, A. O. Inman, *Carbon* **2006**, *44*, 1070.

[18] S. K. Smart, A. I. Cassady, G. Q. Lu, D. J. Martin, *Carbon* **2006**, *44*, 1034.

[19] G. Oberdorster, E. Oberdorster, J. Oberdorster, *Environ. Health Perspect.* **2005**, *113*, 823.

[20] E. Kagan, Y. Y. Tyurina, V. A. Tyurin, N. V. Konduru, A. I. Potapovich, A. N. Osipov, E. R. Kisin, D. Schwegler-Berry, R. Mercer, V. Castranova, A. A. Shvedova, *Toxicol. Lett.* **2006**, *165*, 88.

[21] E. Flahaut, M. C. Durrieu, M. Remy-Zolghadri, R. Bareille, C. Baquey, *Carbon* **2006**, *44*, 1093.

[22] M. L. Becker, J. A. Fagan, N. D. Gallant, B. J. Bauer, V. Bajpai, E. K. Hobbie, S. H. Lacerda, K. B. Migler, J. P. Jakupciak, *Adv. Mater.* **2007**, *19*, 939.

[23] N. W. S. Kam, M. O'Connell, J. A. Wisdom, H. J. Dai, *Proc. Natl. Acad. Sci. U.S.A.* **2005**, *102*, 11600.

[24] R. Singh, D. Pantarotto, L. Lacerda, G. Pastorin, C. Klumpp, M. Prato, A. Bianco, K. Kostarelos, *Proc. Natl. Acad. Sci. U.S.A.* **2006**, *103*, 3357.

[25] Y. Lin, B. Zhou, R. B. Martin, K. B. Henbest, B. A. Harruff, J. E. Riggs, Z. X. Guo, L. F. Allard, Y. P. Sun, *J. Phys. Chem. B* **2005**, *109*, 14779.

[26] D. Pantarotto, R. Singh, D. McCarthy, M. Erhardt, J. P. Briand, M. Prato, K. Kostarelos, A. Bianco, *Angew. Chem. Int. Ed.* **2004**, *43*, 5242.

[27] D. Cai, J. M. Mataraza, Z. H. Qin, Z. P. Huang, J. Y. Huang, T. C. Chiles, D. Carnahan, K. Kempa, Z. F. Ren, *Nat. Methods* **2005**, *2*, 449.

[28] Q. Lu, J. M. Moore, G. Huang, A. S. Mount, A. M. Rao, L. L. Larcom, P. C. Ke, *Nano Lett.* **2004**, *4*, 2473.

[29] S. F. Chin, H. Baughman Ray, B. Dalton Alan, R. Dieckmann Gregg, K. Draper Rockford, C. Mikoryak, H. Musselman Inga, V. Z. Poenitzsch, H. Xie, P. Pantano, *Exp. Biol. Med. (Maywood)* **2007**, *232*, 1236.

[30] J. M. Worle-Knirsch, K. Pulskamp, H. F. Krug, *Nano Lett.* **2006**, *6*, 1261.

[31] S. Garibaldi, C. Brunelli, V. Bavastrello, G. Ghigliotto, C. Nicolini, *Nanotechnology* **2006**, *17*, 391.

[32] X. Chen, U. C. Tam, J. L. Czlapinski, G. S. Lee, D. Rabuka, A. Zettl, C. R. Bertozzi, *J. Am. Chem. Soc.* **2006**, *128*, 6292.

[33] S. Koyama, M. Endo, Y. A. Kim, T. Hayashi, T. Yanagisawa, K. Osaka, H. Koyama, H. Haniu, N. Kuroiwa, *Carbon* **2006**, *44*, 1079.

[34] Y. Zhu, T. Ran, Y. Li, J. Guo, W. Li, *Nanotechnology* **2006**, *17*, 4668.

[35] H. Dumortier, S. Lacotte, G. Pastorin, R. Marega, W. Wu, D. Bonifazi, J. P. Briand, M. Prato, S. Muller, A. Bianco, *Nano Lett.* **2006**, *6*, 1522.

[36] H. Hu, Y. Ni, V. Montana, R. C. Haddon, V. Parpura, *Nano Lett.* **2004**, *4*, 507.

[37] N. A. Monteiro-Riviere, R. J. Nemanich, A. O. Inman, Y. Y. Wang, J. E. Riviere, *Toxicol. Lett.* **2005**, *155*, 377.

[38] G. Jia, H. Wang, L. Yan, X. Wang, R. Pei, T. Yan, Y. Zhao, X. Guo, *Environ. Sci. Technol.* **2005**, *39*, 1378.

[39] A. Shvedova, V. Castranova, E. Kisin, D. Schwegler-Berry, A. Murray, V. Gandelsman, A. Maynard, P. Baron, *J Toxicol. Environ. Health* **2003**, *66*, 1909.

[40] A. Magrez, S. Kasas, V. Salicio, N. Pasquier, J. W. Seo, M. Celio, S. Catsicas, B. Schwaller, L. Forro, *Nano Lett.* **2006**, *6*, 1121.

[41] D. Cui, F. Tian, C. S. Ozkan, M. Wang, H. Gao, *Toxicol. Lett.* **2005**, *155*, 73.

[42] D. B. Warheit, B. R. Laurence, K. L. Reed, D. H. Roach, G. A. M. Reynolds, T. R. Webb, *Toxicol. Sci.* **2004**, *77*, 117.

[43] S. K. Manna, S. Sarkar, J. Barr, K. Wise, E. V. Barrera, O. Jejelowo, A. C. Rice-Ficht, G. T. Ramesh, *Nano Lett.* **2005**, *5*, 1676.

[44] L. Ding, J. Stilwell, T. Zhang, O. Elboudwarej, H. Jiang, J. P. Selegue, P. A. Cooke, J. W. Gray, F. F. Chen, *Nano Lett.* **2005**, *5*, 2448.

[45] C. M. Sayes, F. Liang, J. L. Hudson, J. Mendez, W. Guo, J. M. Beach, V. C. Moore, C. D. Doyle, J. L. West, W. E. Billups, K. D. Ausman, V. L. Colvin, *Toxicol. Lett.* **2006**, *161*, 135.

[46] J. Chlopek, B. Czajkowska, B. Szaraniec, E. Frackowiak, K. Szostak, F. Beguin, *Carbon* **2006**, *44*, 1106.

[47] R. C. Templeton, P. L. Ferguson, K. M. Washburn, W. A. Scrivens, G. T. Chandler, *Environ. Sci. Technol.* **2006**, *40*, 7387.

[48] C. W. Lam, J. T. James, R. McCluskey, R. L. Hunter, *Toxicol. Sci.* **2004**, *77*, 126.

[49] D. B. Warheit, *Carbon* **2006**, *44*, 1064.

[50] C. A. Poland, R. Duffin, I. Kinloch, A. Maynard, W. A. Wallace, A. Seaton, V. Stone, S. Brown, W. Macnee, K. Donaldson, *Nat. Nanotechnol.* **2008**, *3*, 423.

[51] P. Cherukuri, C. J. Gannon, T. K. Leeuw, H. K. Schmidt, R. E. Smalley, S. A. Curley, B. Weisman, *Proc. Natl. Acad. Sci. U.S.A.* **2006**, *103*, 18882.

[52] Z. Liu, W. B. Cai, L. N. He, N. Nakayama, K. Chen, X. M. Sun, X. Y. Chen, H. J. Dai, *Nat. Nanotechnol.* **2007**, *2*, 47.

[53] J. C. G. Jeynes, E. Mendoza, D. C. S. Chow, P. C. R. Watts, J. McFadden, S. R. P. Silva, *Adv. Mater.* **2006**, *18*, 1598.

[54] E. Heister, C. Lamprecht, V. Neves, C. Tilmaciu, L. Datas, E. Flahaut, B. Soula, P. Hinterdorfer, H. M. Coley, S. R. P. Silva, J. McFadden, *ACS Nano* **2010**, *4*, 2615.

[55] D. A. Heller, E. S. Jeng, T. K. Yeung, B. M. Martinez, A. E. Moll, J. B. Gastala, M. S. Strano, *Science* **2006**, *311*, 508.

[56] D. A. Heller, S. Baik, T. E. Eurell, M. S. Strano, *Adv. Mater.* **2005**, *17*, 2793.

[57] C. Krafft, T. Knetschke, A. Siegner, R. H. W. Funk, R. Salzer, *Vib. Spectrosc.* **2003**, *32*, 75.

[58] I. Notingher, S. Verrier, S. Haque, J. M. Polak, L. L. Hench, *Biopolymers* **2003**, *72*, 230.

[59] C. Krafft, T. Knetschke, R. H. W. Funk, R. Salzer, *Vib. Spectrosc.* **2005**, *38*, 85.

[60] M. S. Dresselhaus, G. Dresselhaus, A. Jorio, A. G. Souza Filho, R. Saito, *Carbon* **2002**, *40*, 2043.

[61] P. Puech, A. Ghandour, A. Sapelkin, C. Tinguely, E. Flahaut, D. J. Dunstan, W. Bacsa, *Phys. Rev. B* **2008**, *78*, 045413.

[62] Y. Saito, T. Yoshikawa, S. Bandow, T. Tomita, T. Hayashi, *Phys. Rev. B* **1993**, *48*, 1907.

[63] B. L. Allen, P. D. Kichambare, P. Gou Vlasova II, A. A. Kapralov, N. Konduru, V. E. Kagan, A. Star, *Nano Lett.* **2008**, *8*, 3899.

[64] X. Liu, R. H. Hurt, A. B. Kane, *Carbon* **2010**, *48*, 1961.

[65] S. Verrier, I. Notingher, J. M. Polak, L. L. Hench, *Biopolymers* **2004**, *74*, 157.

[66] G. J. Puppels, H. S. Garritsen, G. M. Segers-Nolten, F. F. de Mul, J. Greve, *Biophys. J.* **1991**, *60*, 1046.

[67] E. Flahaut, R. Bacsa, A. Peigney, C. Laurent, *Chem. Commun.* **2003**, 1442.

[68] E. Heister, V. Neves, C. Tilmaciu, K. Lipert, V. S. Beltran, H. M. Coley, S. R. P. Silva, J. McFadden, *Carbon* **2009**, *47*, 2152.

[69] R. A. Jishi, L. Venkataraman, M. S. Dresselhaus, G. Dresselhaus, *Chem. Phys. Lett.* **1993**, *209*, 77.

[70] S. Cooper, *BMC Cell Biol.* **2004**, *5*, 5.